nature nanotechnology

LETTERS

PUBLISHED ONLINE: 27 JULY 2015 | DOI: 10.1038/NNANO.2015.159

Deterministic photon–emitter coupling in chiral photonic circuits

Immo Söllner[1]*, Sahand Mahmoodian[1], Sofie Lindskov Hansen[1], Leonardo Midolo[1], Alisa Javadi[1], Gabija Kiršanskė[1], Tommaso Pregnolato[1], Haitham El-Ella[1], Eun Hye Lee[2], Jin Dong Song[2], Søren Stobbe[1] and Peter Lodahl[1]*

Engineering photon emission and scattering is central to modern photonics applications ranging from light harvesting to quantum-information processing. To this end, nanophotonic waveguides are well suited as they confine photons to a one-dimensional geometry and thereby increase the light–matter interaction. In a regular waveguide, a quantum emitter interacts equally with photons in either of the two propagation directions. This symmetry is violated in nanophotonic structures in which non-transversal local electric-field components imply that photon emission[1,2] and scattering[3] may become directional. Here we show that the helicity of the optical transition of a quantum emitter determines the direction of single-photon emission in a specially engineered photonic-crystal waveguide. We observe single-photon emission into the waveguide with a directionality that exceeds 90% under conditions in which practically all the emitted photons are coupled to the waveguide. The chiral light–matter interaction enables deterministic and highly directional photon emission for experimentally achievable on-chip non-reciprocal photonic elements. These may serve as key building blocks for single-photon optical diodes, transistors[4] and deterministic quantum gates[5]. Furthermore, chiral photonic circuits allow the dissipative preparation of entangled states of multiple emitters[6] for experimentally achievable parameters[7], may lead to novel topological photon states[8,9] and could be applied for directional steering of light[10–13].

Truly 1D photon/emitter interfaces are desirable for a range of applications in photonic quantum-information processing[14]. To this end, photonic-crystal waveguides constitute an ideal platform that features on-chip integration with the ability to engineer the light–matter coupling. Recent experiments achieved a coupling efficiency for a single quantum dot (QD) to a photonic-crystal waveguide in excess of 98%, which thus constitutes a deterministic 1D photon/emitter interface[15]. Standard photonic-crystal waveguides are mirror symmetric around the centre of the waveguide, and all modes consequently have odd/even symmetry under a reflection in a vertical centre plane. The electric-field maxima are positioned in the centre plane for a standard photonic-crystal waveguide and, as a consequence, the mode polarization is predominantly linear at the positions where the light intensity is high[14,15] (see the Supplementary Information for more details). Therefore, breaking this symmetry is required to engineer modes that are circularly polarized at the field maxima. An ideal way to break the reflection symmetry is by shifting one side of the waveguide by half a lattice constant, which is referred to as a glide-plane waveguide (GPW) (see the Supplementary Information for further descriptions of the structure). In a GPW, a QD with a circularly polarized transition dipole emits preferentially in a single direction. The direction is determined by the helicity (see Fig. 1a), and the exact branching ratio between the two emission directions depends on the position of the QD. The two figures-of-merit for chiral single-photon emission are displayed in Fig. 1b,c. They are the fraction of photons emitted into the waveguide that propagates in a desired direction (F_{dir}) and the overall probability that an emitted photon from the QD is channelled into the correct direction (β_{dir}). The GPW is engineered to increase the β factor and features $\beta_{\mathrm{dir}} = 98\%$ (see Fig. 1c), which enables the deterministic interfacing of single emitters and single photons. An ideal directional photon/emitter interface corresponds to $\beta_{\mathrm{dir}} \to 1$, which probably can be achieved by further engineering of the GPW. We emphasize the robustness of the directional coupling, because the GPW is designed to have a highly directional coupling within a large region of each unit cell of the photonic-crystal waveguide. The present work reports on the observation of highly directional emission at the single-photon level by efficiently coupling a single QD to a GPW. We show that this is the basic operational principle required to construct non-reciprocal elements based on chiral photonic circuits.

Figure 1d displays a scanning electron microscope (SEM) image of our photonic waveguide and illustrates the directional coupling. Single self-assembled QDs in the GPW are excited optically and two non-degenerate circularly polarized exciton states, $|+\rangle$ and $|-\rangle$ (see Fig. 1a), are formed by applying a strong magnetic field (B_z) in the QD growth direction[16]. By non-resonant optical excitation, a statistical mixture of the two exciton states is prepared that can decay to the ground state via $\Delta m = \pm 1$ dipole transitions that emit $\sigma_{\pm}$ polarized photons. These QD transitions are used to demonstrate chiral photon emission. The origin of the chiral interaction can be understood as follows: from time-reversal symmetry, the electric fields, $\mathbf{E}$, of counter-propagating modes with wave vectors k and $-k$ satisfy $\mathbf{E}_{-k}(\mathbf{r}) = \mathbf{E}_{k}^{*}(\mathbf{r})$, that is, for a mode with an in-plane circular polarization at position $\mathbf{r}$, the counter-propagating mode has the orthogonal circular polarization. As a circularly polarized emitter only couples to the mode that has the same circular polarization as the dipole transition, this leads to unidirectional emission.

An important advantage of photonic crystals is that they allow the interaction between light and matter to be tailored. In a GPW, the chirality is engineered by the structural parameters and depends on the magnitude of the projection of the local electric field onto the QD transition dipole moment (see Fig. 1b,c). The experimental proof of directional emission is obtained by collecting single photons emitted from the QDs by two separate outcoupling gratings at each end of the GPW (see Fig. 1d). We extract the directionality factor F_{dir} by comparing the intensity of one circular dipole to the orthogonal dipole by collecting the intensity from the same

[1]Niels Bohr Institute, University of Copenhagen, Blegdamsvej 17, Copenhagen DK-2100, Denmark. [2]Center for Opto-Electronic Convergence Systems, Korea Institute of Science and Technology, Seoul 136-791, Korea. *e-mail: sollner@nbi.ku.dk; lodahl@nbi.ku.dk

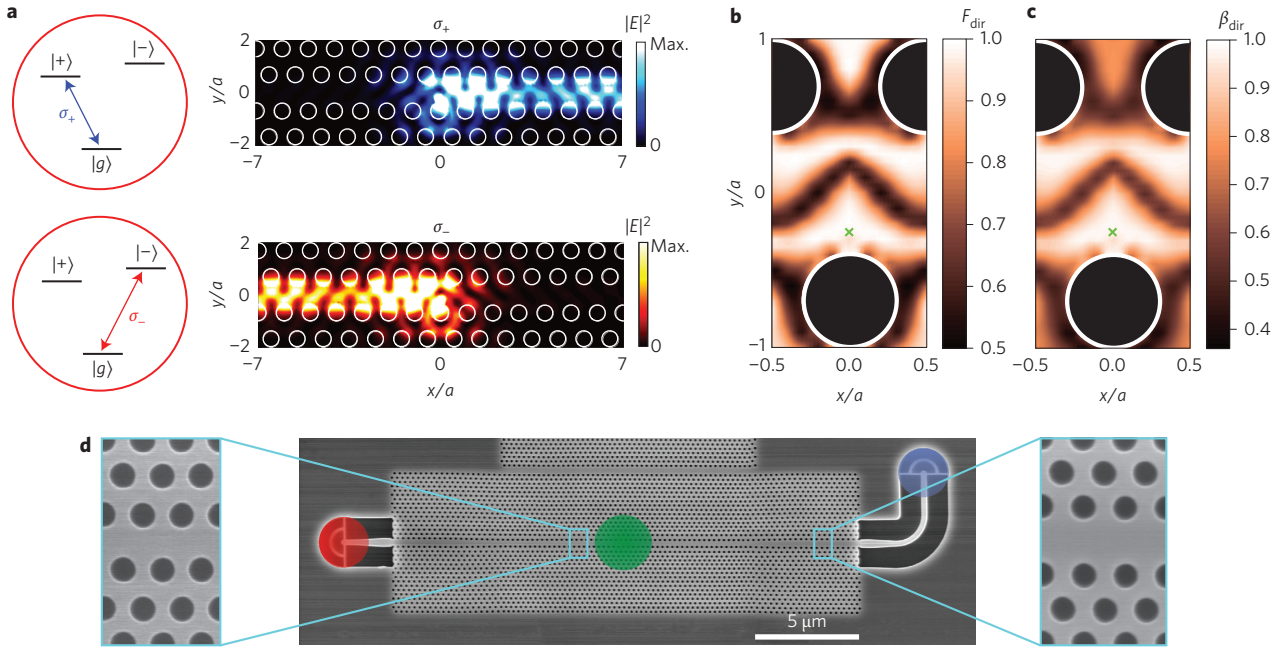

Figure 1 | Operational principle of chiral single-photon emission in a waveguide. a, Left: QD-level scheme in the presence of a magnetic field in the growth directions that features two circularly polarized exciton transitions $\sigma_{\pm}$ with a splitting controlled by the magnetic field. Right: calculated directional emission patterns of σ_+ and σ_- polarized dipole emitters in GPWs. The positions of the dipoles are indicated by the crosses in **b** and **c**. **b**,**c**, Directionality (**b**) and directional β factor (**c**) as a function of position for the GPW mode studied in the experiments. Here, a is the lattice constant of the photonic crystal. **d**, SEM image of the GPW. A QD is excited in the centre of the structure (green area) and photons are collected from the outcoupling gratings at each side of the GPW (red and blue areas). The zoom-ins show the structure of the photonic-crystal lattice that consists of a GPW section (left image) and a standard photonic-crystal waveguide section (right image). The waveguide gradually changes from a glide-plane lattice to a standard lattice to obtain an efficient outcoupling of photons (for the details, see the Supplementary Information).

waveguide ends, which makes the method insensitive to potentially different outcoupling efficiencies at the two ends (see the Supplementary Information). By spectrally resolving the emission, single QD lines are selected and photon correlation measurements are employed to identify separate QDs and quantify the single-photon nature of the emission.

The directionality of the photon emission is extracted from the emission spectra measured for different applied magnetic field strengths (see Fig. 2a–c) and two QD lines (A and B) are studied in detail. Without a magnetic field, the spectra recorded from the two ends of the GPW are almost identical. By increasing the magnetic field, the individual QD lines split into pairs that correspond to the two circularly polarized transitions. Highly directional emission is evident for the peaks labelled B_+ and B_-. Furthermore, Fig. 2b,c show that the two transitions maintain their directionality when changing the polarity of the magnetic field, which swaps the spectral position of orthogonally polarized emission lines. This demonstrates explicitly that the directionality is related to the helicity of the dipole transition.

Figure 2d shows a plot of the directionality of the two QD lines as a function of the applied magnetic field strength. At low magnetic fields the emission lines are not separated clearly, which leads to a systematic underestimation of the directionality factor. At approximately 1 T the directionality levels off and we extract $F_{\mathrm{dir}} = 90 \pm 1.3\%$ for QD B by averaging over the plateau region in Fig. 2d. The lower directionality of QD A stems from the spatial variation within the unit cell of the GPW (see Fig. 1b). The extracted directionality constitutes a lower bound of the actual value because of the presence of weak emission from transitions other than the investigated QD, which is a result of the non-resonant excitation method applied in the experiment. In addition, the presence of residual reflections at the outcoupling gratings further limits the experimentally extracted value. Consequently, the actual directionality for the single QD transition is likely to approach unity, in accordance with theory (Fig. 1b). The single-photon nature of the emission can be proved through correlation measurements (see Fig. 2e). A pronounced antibunching is observed for peaks A and B, which illustrates that high-purity single-photon emission is observed. Furthermore, the absence of correlations in the cross-correlation measurement between A and B shows that the two peaks originate from two independent QDs.

A major asset of the photonic-crystal waveguide platform is that the light–matter interaction can be controlled to such a degree that the photon/emitter interface becomes deterministic[14], as is quantified by the β factor. In time-resolved measurements, we recorded a decay rate of $0.80 \pm 0.02\ \mathrm{ns}^{-1}$ for QD B. This restricts the possible spatial position of the QD as well as its spectral position relative to the photonic waveguide bands of the GPW. From numerical calculations, we estimate an upper bound on the rate at which the QD leaks to non-guided modes, and also, by accounting for the contribution from intrinsic non-radiative decay processes of the QD, we arrive at $\beta \gtrsim 90\%$. The detailed measurements of the β factor in standard photonic-crystal waveguides are presented in Arcari *et al.*[15].

Having demonstrated the basic operational principle of deterministic chiral photon emission, this functionality can be exploited for the construction of non-reciprocal photonic elements, such as single-photon diodes and circulators. The architecture is based on a QD coupled to a GPW, which is placed in one arm of a Mach–Zehnder interferometer (MZI) (see Fig. 3a). We consider the scattering by a singly charged QD initially prepared in the spin-up state[18]. A resonant narrow-band single photon (blue wave packet) scatters off the QD transition and obtains a π-phase shift[19] (see the Supplementary Information for the calculations). (The acquired

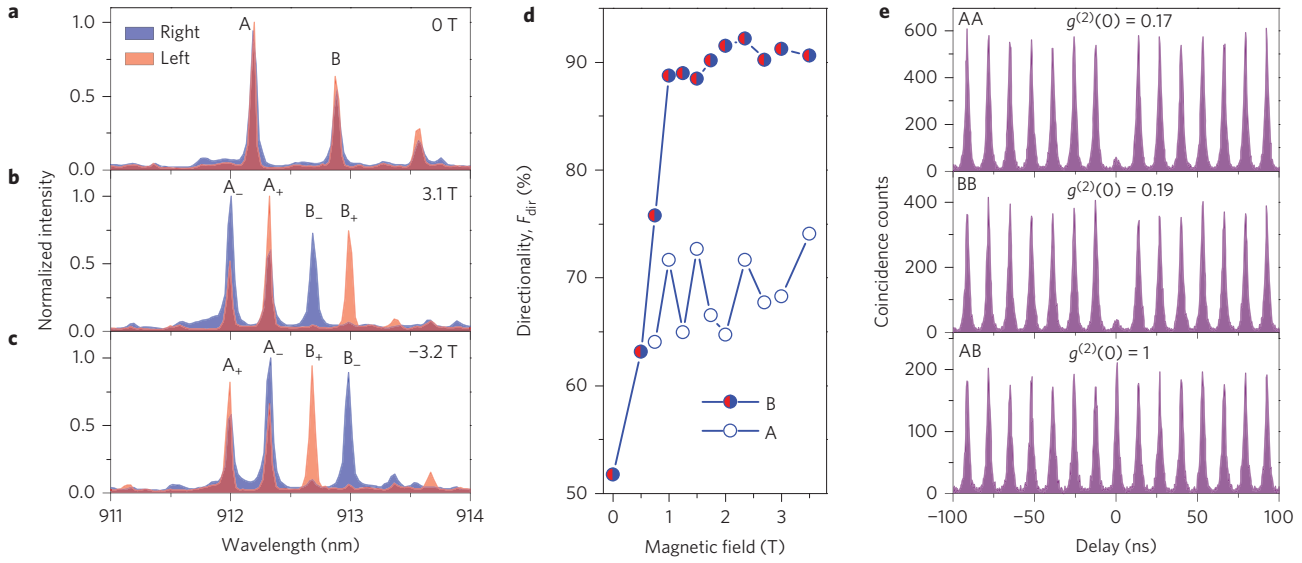

Figure 2 | Observation of directional emission of single QDs in a GPW. a, Emission spectra that display two different QD lines, denoted A and B, that are recorded on the right (blue spectrum) or the left (red spectrum) grating outcoupler. **b**, By applying a magnetic field the QD lines split into duplets $A_{\pm}$ and $B_{\pm}$ that display different directionalities. **c**, Emission spectra recorded for a negative magnetic field. For the opposite polarity the two exciton lines swap spectral position, with the directional outcoupling preserved. **d**, Extracted directionality for QD A and B as a function of the applied magnetic field. At low magnetic fields the lines B_- and B_+ are not sufficiently separated, which leads to a systematic underestimate of the directionality factor. At approximately 1 T the directionality levels off and stays constant for the entire range of magnetic fields investigated. An average directionality factor of $F_{dir} = 90 \pm 1.3\%$ was obtained for QD B. **e**, Demonstration of the single-photon operation of the chiral waveguide. AA (BB) denotes correlation measurements on QD line A (B) coupled out from the two separate ends of the GPW. The single-photon purity of the emission is quantified by extracting $g^{(2)}(0)$ from the data[17], where $g^{(2)}(0) < 1/2$ is the distinct antibunching signature of single-photon emission. AB denotes a cross-correlation between the two QD lines A and B. The lack of any correlations proves that A and B correspond to two independent QDs. The data were taken at 0 T.

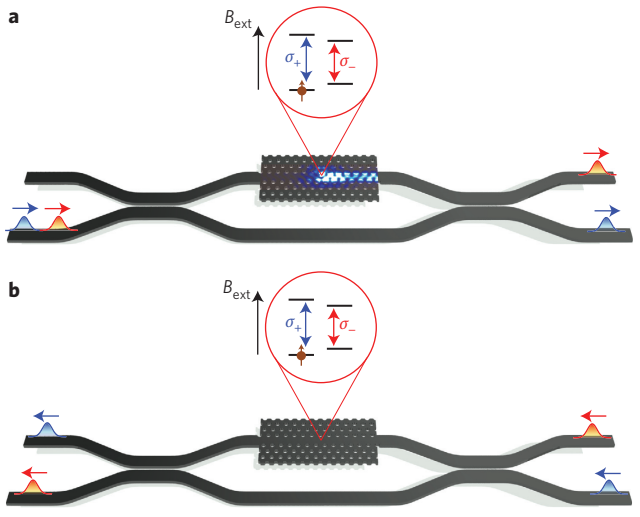

Figure 3 | Non-reciprocal transport of photons in a chiral photonic circuit. **a**, The non-reciprocal element consists of an on-chip MZI with a singly charged QD coupled to a GPW in one of the arms. A resonant photon (blue) injected from the left scatters off the QD in the top arm and accumulates a π-phase shift relative to the case in which no interaction takes place. This leads the photon to exit the MZI in the bottom arm. A photon resonant on the other transition (red) does not interact with the QD and thus exits in the upper arm. **b**, In the time-reversed case the two photons enter from the right of the MZI and neither photon interacts with the QD because the left propagating mode is orthogonal to the σ_+ transition.

transmission coefficient is at variance with the results reported in Shen *et al.*[20]. This mistake was communicated to and acknowledged by Shen and co-workers.) The MZI is balanced so that incident photons entering in the bottom arm exit through the bottom arm if they obtain a π-phase shift. A non-resonant photon (red wave packet) does not interact with the QD and exits the top arm. It follows that the spin of the ground state completely determines the output arm from which the resonant photon exits the MZI, constituting an on-chip spin readout. Next, we consider the reciprocal case in which the two photons are directed back into the MZI, as shown in Fig. 3b. Now the resonant photon does not interact with the QD, as the left propagating mode is orthogonal to the σ_+ transition and exits the top arm. This non-reciprocal transport is caused by a single spin in the QD, which constitutes a giant magneto-optical effect. The GPW-integrated MZI can form the basis for several quantum applications, and adding the coherent control of the QD spin state allows for the creation of a deterministic controlled NOT gate for photons (see the Supplementary Information for more details).

Finally, it is interesting that the non-reciprocal transport of light constitutes a violation of the time-reversal symmetry of the optical field. Breaking time-reversal symmetry is a necessary condition to obtain topologically non-trivial photonic quantum Hall states[21]. The use of a single quantum emitter as a non-reciprocal element implies that the response of the entire system is highly nonlinear, that is, the behaviour strongly depends on whether a single photon or two photons are considered. This may allow the study of nonlinear optical transport in topological systems and the creation of novel photon–photon bound states.

A chiral photon/emitter interface represents a novel way to couple deterministically single quanta of light and matter. It is expected to have widespread applications for scalable quantum-information processing that utilizes photons. The general principle of engineering chiral interactions can very probably be extended to platforms other than those considered here, for instance to the case of atoms in photonic-crystal structures[22,23], colour centres in diamonds[24,25] or superconducting qubits[26].

Methods

Methods and any associated references are available in the online version of the paper.

Received 7 December 2014; accepted 22 June 2015; published online 27 July 2015

References

1. Mitsch, R., Sayrin, C., Albrecht, B., Schneeweiss, P. & Rauschenbeutel, A. Quantum state-controlled directional spontaneous emission of photons into a nanophotonic waveguide. *Nature Commun.* **5,** 5713 (2014).
2. Luxmoore, I. J. *et al.* Interfacing spins in an InGaAs quantum dot to a semiconductor waveguide circuit using emitted photons. *Phys. Rev. Lett.* **110,** 037402 (2013).
3. Junge, C., O'Shea, D., Volz, J. & Rauschenbeutel, A. Strong coupling between single atoms and nontransversal photons. *Phys. Rev. Lett.* **110,** 213604 (2013).
4. Chang, D. E., Sørensen, A. S., Demler, E. A. & Lukin, M. D. A single-photon transistor using nanoscale surface plasmons. *Nature Phys.* **3,** 807–812 (2007).
5. Duan, L. M. & Kimble, H. J. Scalable photonic quantum computation through cavity-assisted interactions. *Phys. Rev. Lett.* **92,** 127902 (2004).
6. Stannigel, K., Rabl, P. & Zoller, P. Driven-dissipative preparation of entangled states in cascaded quantum-optical networks. *New J. Phys.* **14,** 063014 (2012).
7. Ramos, T., Pichler, H., Daley, A. J. & Zoller, P. Quantum spin dimers from chiral dissipation in cold-atom chains. *Phys. Rev. Lett.* **113,** 237203 (2014).
8. Hafezi, M., Demler, E. A., Lukin, M. D. & Taylor, J. M. Robust optical delay lines with topological protection. *Nature Phys.* **7,** 907–912 (2010).
9. Kraus, Y. E., Lahini, Y., Ringel, Z., Verbin, M. & Zilberberg, O. Topological states and adiabatic pumping in quasicrystals. *Phys. Rev. Lett.* **109,** 106402 (2012).
10. Rodriguez-Fortuño, F. J. *et al.* Near-field interference for the unidirectional excitation of electromagnetic guided modes. *Science* **340,** 328–330 (2013).
11. Petersen, J., Volz, J. & Rauschenbeutel, A. Chiral nanophotonic waveguide interface based on spin–orbit interaction of light. *Science* **346,** 67–71 (2014).
12. Neugebauer, M., Bauer, T., Banzer, P. & Leuchs, G. Polarization tailored light driven directional optical nanobeacon. *Nano Lett.* **14,** 2546–2551 (2014).
13. le Feber, B., Rotenberg, N. & Kuipers, L. Nanophotonic control of circular dipole emission. *Nature Commun.* **6,** 6695 (2015).
14. Lodahl, P., Mahmoodian, S. & Stobbe, S. Interfacing single photons and single quantum dots with photonic nanostructures. *Rev. Mod. Phys.* **87,** 347–400 (2015).
15. Arcari, M. *et al.* Near-unity coupling efficiency of a quantum emitter to a photonic crystal waveguide. *Phys. Rev. Lett.* **113,** 093603 (2014).
16. Bayer, M. *et al.* Fine structure of neutral and charged excitons in self-assembled In(Ga)As/(Al)GaAs quantum dots. *Phys. Rev. B* **65,** 195315 (2002).
17. Santori, C., Fattal, D. & Yamamoto, Y. *Single-Photon Devices and Applications* (John Wiley & Sons, Inc., 2010).
18. Yilmaz, S. T., Fallahi, P. & Imamoglu, A. Quantum-dot-spin single-photon interface. *Phys. Rev. Lett.* **105,** 033601 (2010).
19. Fan, S., Kocabaş, Ş. E. & Shen, J.-T. Input–output formalism for few-photon transport in one-dimensional nanophotonic waveguides coupled to a qubit. *Phys. Rev. A* **82,** 063821 (2010).
20. Shen, Y., Bradford, M. & Shen, J.-T. Single-photon diode by exploiting the photon polarization in a waveguide. *Phys. Rev. Lett.* **107,** 173902 (2011).
21. Lu, L., Joannopoulos, J. D. & Soljačić, M. Topological photonics. *Nature Photon.* **8,** 821–829 (2014).
22. Tiecke, T. G. *et al.* Nanophotonic quantum phase switch with a single atom. *Nature* **508,** 241–244 (2014).
23. Goban, A. *et al.* Atom–light interactions in photonic crystals. *Nature Commun.* **5,** 4808 (2014).
24. Riedrich-Möller, J. *et al.* Deterministic coupling of a single silicon-vacancy color center to a photonic crystal cavity in diamond. *Nano Lett.* **14,** 5281–5287 (2014).
25. Li, L. *et al.* Coherent spin control of a nanocavity-enhanced qubit in diamond. *Nature Commun.* **6,** 6173 (2015).
26. Hoi, I.-C. *et al.* Generation of nonclassical microwave states using an artificial atom in 1D open space. *Phys. Rev. Lett.* **108,** 263601 (2012).

Acknowledgements

We thank A. Sørensen and D. Witthaut for valuable discussions and gratefully acknowledge financial support from the Villum Foundation, the Carlsberg Foundation, the Danish Council for Independent Research (Natural Sciences and Technology and Production Sciences), and the European Research Council (ERC Consolidator Grant ALLQUANTUM). E.H.L. and J.D.S. acknowledge support from the Global Research Lab and the Flagship Program (Korea Institute of Science and Technology).

Author contributions

I.S. and S.M. designed the experiment and analysed the data. S.M. and A.J. performed the numerical simulations. I.S. and S.L.H. carried out the experiments. L.M., G.K., T.P. and H.E. fabricated the sample. E.H.L. and J.D.S. grew the semiconductor material. P.L. and S.S. supervised the project. P.L., S.S., S.M. and I.S. wrote the manuscript with input from all the authors.

Additional information

Supplementary information is available in the online version of the paper. Reprints and permissions information is available online at www.nature.com/reprints. Correspondence and requests for materials should be addressed to I.S. and P.L.

Competing financial interests

The authors declare no competing financial interests.

Methods

Sample. The sample was grown by molecular beam epitaxy on an undoped (100) GaAs substrate. A 160 nm thick GaAs membrane was grown on a 1.42 μm thick $Al_{0.75}Ga_{0.25}As$ sacrificial layer. The membrane contained a single layer of low-density self-assembled In(Ga)As QDs, and emitted around 920 nm at 10 K (density $\simeq 50\ \mu m^{-2}$). The photonic nanostructures were patterned by electron-beam lithography at 100 keV on a 500 nm thick electron beam resist (ZEP 520A) and aligned to the [011] or [0–11] directions of the GaAs substrate. The photonic-crystal holes were etched by an inductively coupled plasma in a $BCl_3/Cl_2/Ar$ chemistry at 0 °C. The remaining photoresist was stripped using hot *N*-methyl-2-pyrrolidone and the membranes were subsequently released in a wet-etching step, which removed the AlGaAs sacrificial layer using a hydrofluoric acid solution (10% w/w).

Experiment. The measurements were performed in a helium-bath cryostat operating at 4.2 K. The samples were mounted on a stack of piezoelectric nanopositioning stages that allowed for a precise positioning of the sample with respect to the objective. A superconducting coil was able to generate magnetic fields up to 9 T and surrounded the stage and sample such that the generated field pointed along the QD growth direction. The QDs were optically pumped by a Ti:sapphire laser at an emission wavelength of 842 nm. The laser was operated in the continuous-wave mode for the spectral measurements and in the pulsed mode (3 ps pulses at a repetition rate of 76 MHz) for lifetime and correlation measurements. Both excitation and collection were performed through the same microscope objective (numerical aperture, 0.65). The excitation beam was moved to the centre of the waveguide and the emission was collected from both gratings at the same time. The emission from the two gratings was coupled into separate single-mode polarization-maintaining fibres that each led to their own spectrometer set-up (1,200 grooves mm^{-1} grating), where avalanche photodiodes were used for time-resolved measurements, and a charge-coupled device was used to record the spectra.